Supporting Information

Origin of the Overpotentials for HCOO⁻ and CO Formation in the Electroreduction of CO_2 on Cu(211): the Reductive Desorption Processes Decide

Ling Liu and Chungen Liu*

Institute of Theoretical and Computational Chemistry, Key Laboratory of Mesoscopic Chemistry of the Ministry of Education (MOE), School of Chemistry and Chemical Engineering, Nanjing University, Nanjing, 210023, China

E-mail: cgliu@nju.edu.cn

Convergence test

Through a few preliminary computations, we found that adopting a loosen force threshold (0.05 eV/Å for structural optimization and 0.1 eV/Å for CINEB) can reasonably reproduce the equilibrium geometries, accordingly, the errors in the energies are within 0.03 eV, which should be acceptable considering the accuracy of the present generation of DFT methods.

Table S1: Discrepancies in the DFT energies, between the results computed with the adopted scheme (0.1 eV/Å, CINEB with 6 images) and those with several other schemes (in units of eV).

	System charge	CINEB, 0.05 eV/Å		Dimer	
	q/e	6 images	8 images	0.05 eV/Å	0.02 eV/Å
TS1	0.0	-0.00076	-0.00162	-0.00001	-0.00239
	-1.0	-0.00321	-0.00364	-0.00274	-0.00504
TS3	0.0	-0.01776	-0.00050	0.00033	-0.00103
	-1.0	-0.00105	-0.00151	-0.00000	-0.00122

Listed in Table S1 are the demonstrative results concerning two transition states, one is in the hydrogenation step of the $HCOO^-$ pathway (TS1), and the other is in the CO_2 chemisorption step of the CO pathway (TS3). Each transition state was optimized at two electrochemical potentials (by introducing in $0.0e$ and $-1.0e$ system charges, respectively). Energies obtained with 0.1 eV/Å as the force threshold are compared against those with 0.05 eV, and 0.02 eV/Å (transition state geometries were further refined with the dimer method after CINEB calculations). It could be found that the discrepancies in energy from these computational schemes are always less than 0.02 eV.

Table S2: Discrepancies in the DFT energies, between the results computed with the adopted 0.05 eV/Å and those with 0.02 eV/Å convergence criterion of force.

	CO_2*+H*		*uni*-HCOO*	
Charge q/e	0.0	-1.0	0.0	-1.0
$\Delta E(0.02)$	-0.02094	-0.00475	-0.00696	-0.00922
	CO_2*		*$CO_2^{\delta-}$	
Charge q/e	0.0	-1.0	0.0	-1.0
$\Delta E(0.02)$	-0.00039	-0.00886	-0.00213	-0.01133

Listed in Table S2 are the results of the connected reactants and products for TS1 and TS3. The

structures were reoptimized with the forces converged to 0.02 eV/Å . The energy differences from those with the adopted 0.05 eV/Å are calculated to be within 0.03 eV, marked as "$\Delta E(0.02)$" in the table.

Table S3: Thermal correction to the free energy calculated with the adopted scheme (force thresholds are set to 0.05 and 0.1 eV/Å for minimized geometries and transition states, respectively), in comparison with those computed by setting the threshold to 0.02 eV/Å(in units of eV). The temperature is set to 298.15 K.

	CO_2*+H*	TS1	*uni*-HCOO*	CO_2*	TS3	*$CO_2^{\delta-}$
This work	0.30984	0.28482	0.41451	0.13943	0.13400	0.12875
0.02 eV/Å	0.33013	0.27097	0.41194	0.14159	0.11088	0.13371
Discrepancy	0.02028	-0.01386	-0.00257	0.00216	-0.02312	0.00495

Besides, the effects of the convergence on the vibration properties were also test. Thermal correction to the free energy, composed of the entropy corrections ($T\Delta S$) as well as the zero-point vibrational energy (ZPE), had been roughly evaluated through frequency analysis on the adsorbates (fixing all the Cu atoms in the substrate). We listed the discrepancies in the thermal correction terms in Table S3. Obviously, the largest discrepancy in the thermal correction terms is less than 0.025 eV.

Configurations

Figure S1-S2 show the optimized structures along HCOO$^-$ (Path I) and CO pathways (Path II) in the zero-charge system. The upper and lower sets of figures are the side and top views of the surface, respectively.
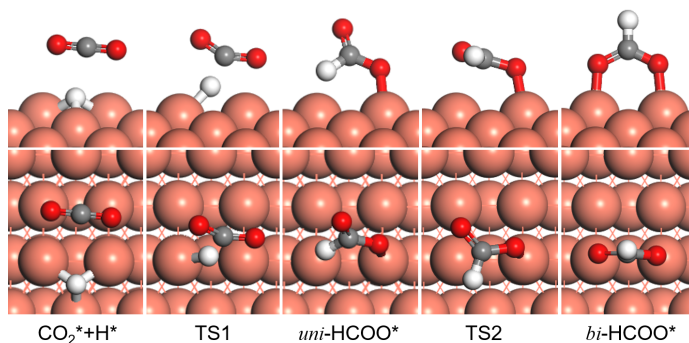

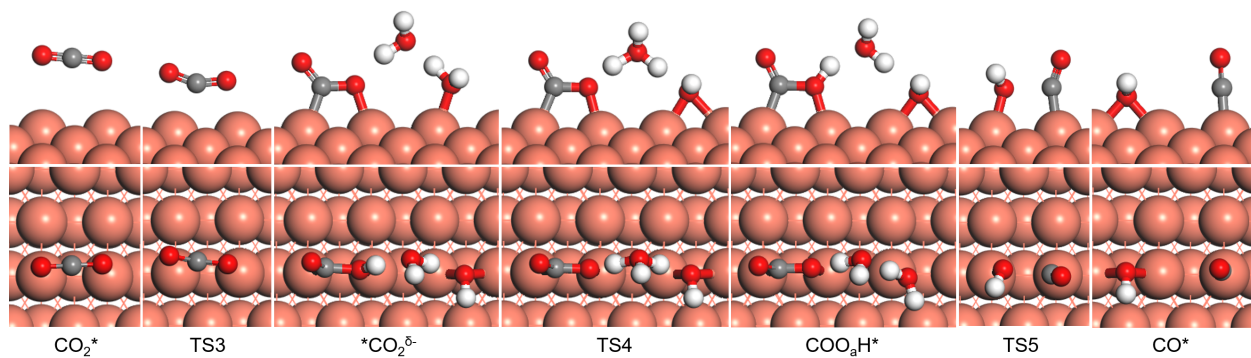Figure S1: Configurations of critical states along reaction route Path I

Figure S2: Configurations of critical states along reaction route Path II

Free energy curves

Figure S3-S6 show potential dependence of the free energies of all critical structures in Path I and Path II. Numbers at the points denote the amount of surface charge in the slab, in units of e.
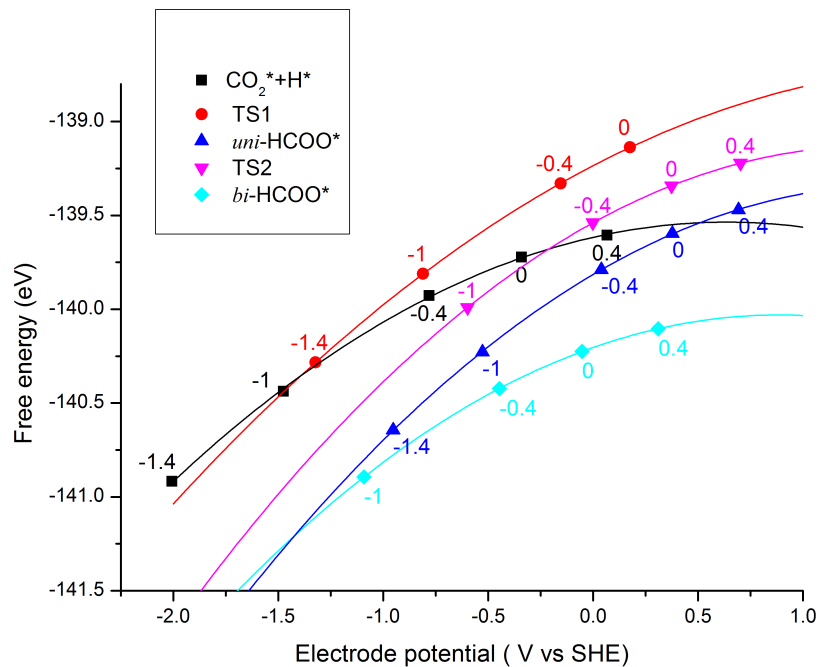
Figure S3: Potential dependence of free energies of all critical structures in Path I.
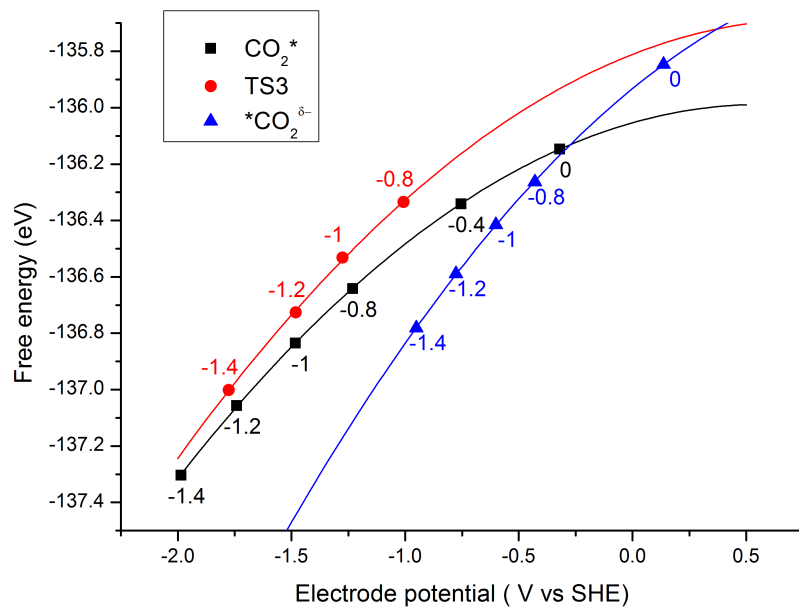

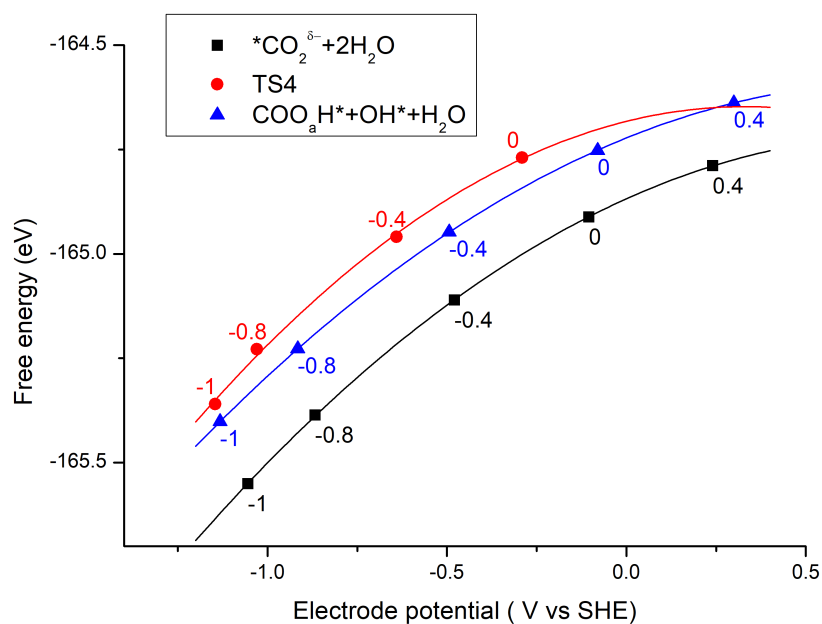Figure S4: Potential dependence of free energies of all critical structures in Path II, part 1.

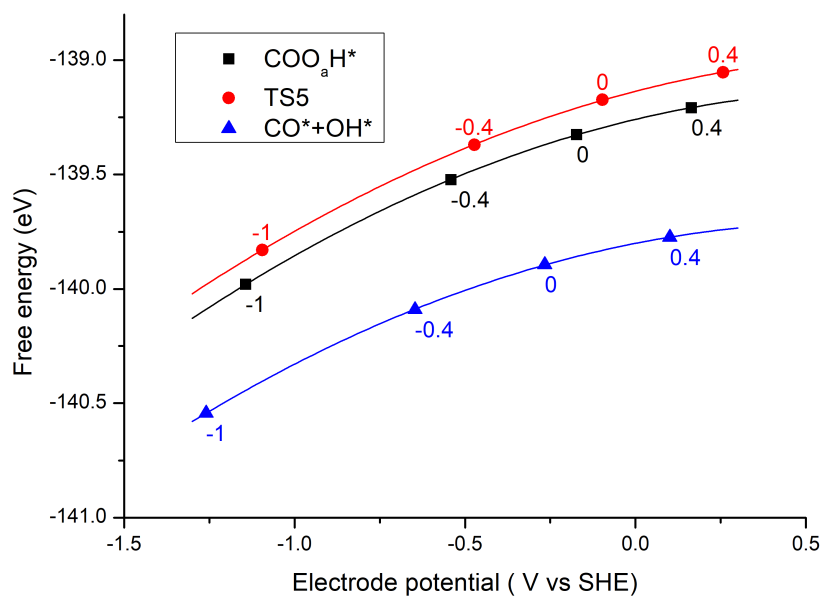Figure S5: Potential dependence of free energies of all critical structures in Path II, part 2.

Figure S6: Potential dependence of free energies of all critical structures in Path II, part 3.